

# Link Level Simulation of MHN-E System

Sung-Woo Choi, Ilgyu Kim

Future Mobile Communication Research Division, ETRI, Daejeon, Rep. of Korea  
csw9908@etri.re.kr, igkim@etri.re.kr

**Abstract**— This paper shows the link level simulation results of the MHN-E system, an enhanced mobile hotspot network system. MHN-E upgraded the specification to obtain twice the data throughput than MHN. The simulator was designed with a fixed-point level and used as a reference for hardware production. We confirmed the transmission performance of MHN-E system in SM mode and SFBC mode through simulation. The performance of the newly adopted polarized antenna is analyzed in cross-permeation condition of the antennas. The experimental result of this paper can be used as a criterion for generating the CQI from the terminal to the base station. The accurate CQI transmission can control the transmission rate according to the downlink channel conditions, thereby improving the overall data throughput.

**Keywords**— millimeter-wave communication, mobile wireless backhaul, link level simulation

## I. INTRODUCTION

With the spread of personal communication terminals represented by smartphones and tablet PCs, people are hoping to access the Internet anytime and anywhere and enjoy various contents. Therefore, Wi-Fi APs are installed in public places where homes, workplaces, schools, and the public gather to provide Internet services. The demand for such Wi-Fi is no exception to public transportation such as subways, buses, and trains, and technology is being actively developed to provide passengers with good quality Wi-Fi services. Among them, Wi-Fi APs in trains are connected to the network using existing wireless communication technologies. At this time, LTE or WiMax is used as a mobile wireless backhaul technology that connects the internal AP of the train to the existing network [1]. However, WiMax backhaul has a maximum data rate of 10 Mbps, and LTE-based backhaul is already using popular technology, so the maximum data rate is expected to be about 100 ~ 200 Mbps [2]. If the number of passengers in the train increases, the transmission rate of the Internet service becomes poor.

Recently, mobile hotspot network (MHN) technology has been developed as a backhaul technology for railway communication [2-5]. Figure 1 illustrates the system architecture of MHN. The train is equipped with a terminal (TE) and forms a radio link with the radio unit (RU), which is a railroad antenna. The RU is connected to the digital unit (DU) through the optical cable, which performs Layer-1 signal processing and L2 / L3 upper layer processing. A DU is connected to an RU one-to-one, and many DU boards are

loaded on the DU RACK. DU boards handle the handover and connect to the Internet through the gateway. The MHN Phase 1 technology has a transmission rate of 1 Gbps using a bandwidth of less than 500 MHz and will be used for the Seoul subway. MHN-E technology was developed to increase the transmission capacity of MHN technology. MHN-E technology basically has a transmission capacity twice as high as that of MHN, and has a transmission rate of 4 times or more according to the frequency bandwidth. ETRI developed the MHN-E prototype system in early 2018 and demonstrated it in the road environment. Demo shows data rates of up to 5 Gbps using a TE mounted on the bus.

The 2x2 spatial multiplexing (SM) transmission is major improvement of MHN-E, so verification of the feasibility of that mode is very important. This paper presents the performance simulation results of downlink of MHN-E prototype system, including SM mode. In the simulation, the influence of cross-permeation component of polarization antenna will be analyzed. The simulator of this paper is developed as a fixed point level and used as a basis for actual hardware development. Therefore, the simulation results show the performance of the actual MHN-E system.

The composition of this paper is as follows. This paper introduces the features of the MHN-E standard in Section II and describes the demodulation algorithm of the terminal receiver. Chapter III briefly describes the structure of the MHN-E TE platform. Section IV then describes the environment and parameters for MHN-E simulation and shows simulation results. Finally, Section V provides some conclusion remarks.

## II. MHN-E SYSTEM

### A. Specification

The MHN-E standard uses most of the main physical layer parameters of MHN as it is. The signal transmission method of the MHN is OFDM, and performs modulation / demodulation using a 1024-point IFFT / FFT. Other major physical layer parameters are listed in Table I. MHN specifications and experimental results have already been covered in other papers [2-6]. This chapter focuses on the differences between MHN and MHN-E standards.

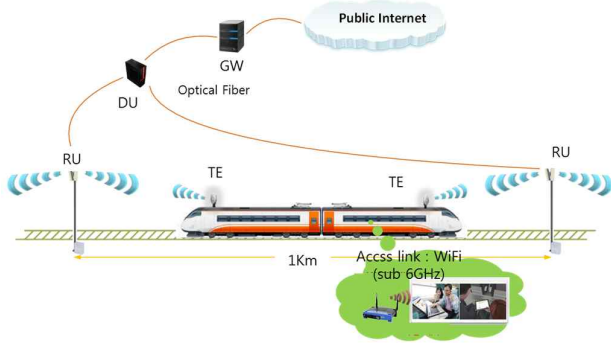


Fig. 1. System architecture of MHN. DU: Digital Unit, RU: Radio Unit, TE: Terminal Equipment, GW: Gateway.

The MHN standard supports 2x2 antennas in the downlink, and has a diversity effect using space frequency block coding (SFBC). The MHN-E standard adds a 2x2 spatial multiplexing (SM) scheme to transmit two independent data streams to it. Therefore, the MHN-E system has a transmission capacity twice that of MHN. MHN-E considered using a polarized antenna for spatial multiplexing. The millimeter wave signal is advantageous for polarized wave communication because it has strong linearity [7]. The use of polarized antennas in wireless communications has already been applied. MHN-E attempts to obtain the multiplexing effect through independent links between antennas by arranging two polarized antennas rotated 90 degrees.

In the spatial multiplexing mode, different data is allocated to independent layers as follows. When signals are transmitted at two antenna ports,  $p \in \{0,1\}$ , the precoding signal for the antenna,  $y(i) = [y^{(0)}(i) \ y^{(1)}(i)]^T$ , is as follows.

$$\begin{bmatrix} y^{(0)}(i) \\ y^{(1)}(i) \end{bmatrix} = \frac{1}{\sqrt{2}} \begin{bmatrix} 1 & 0 \\ 0 & 1 \end{bmatrix} \begin{bmatrix} x^{(0)}(i) \\ x^{(1)}(i) \end{bmatrix} \quad (1)$$

for  $i = 0, 1, \dots, M_{\text{symp}}^{\text{layer}} - 1$

where  $M_{\text{symp}}^{\text{layer}}$  is the number of symbols modulated when one codeword is transmitted over the physical channel.

The SFBC mode, which has good demodulation performance, is used for stable performance even if it has a low data rate. In general, important data such as system information is transmitted in SFBC mode. The precoding output signal in the SFBC mode is as follows.

$$\begin{bmatrix} y^{(0)}(2i) \\ y^{(1)}(2i) \\ y^{(0)}(2i+1) \\ y^{(1)}(2i+1) \end{bmatrix} = \frac{1}{\sqrt{2}} \begin{bmatrix} 1 & 0 & j & 0 \\ 0 & -1 & 0 & j \\ 0 & 1 & 0 & j \\ 1 & 0 & -j & 0 \end{bmatrix} \begin{bmatrix} \text{Re}(x^{(0)}(i)) \\ \text{Re}(x^{(1)}(i)) \\ \text{Im}(x^{(0)}(i)) \\ \text{Im}(x^{(1)}(i)) \end{bmatrix} \quad (2)$$

for  $i = 0, 1, \dots, M_{\text{symp}}^{\text{layer}} - 1$

TABLE I. SUMMARY OF PHYSICAL LAYER SPECIFICATION

Parameters	Value
Size of FFT	1024
Subcarrier spacing	180 kHz
Sampling frequency	184.32 MHz
Cyclic prefix	0.59 $\mu$ s
Symbol duration	6.25 $\mu$ s
Number of OFDM symbols in a slot	40
Channel coding	Turbo Decoding
MIMO (Downlink)	SFBC, Spatial multiplexing
Modulation	QPSK, 16QAM, 64QAM
Sub-band bandwidth	125 MHz

TABLE II. DCI FORMATS OF MHN-E

Format	Usage	bits
DCI 0	uplink scheduling	23
DCI 1	1 TB downlink scheduling	29
DCI 2	2 TB downlink scheduling	34

In the TE, the two modes are determined through the downlink control channel transmitted in the same slot. Therefore, the MHN-E standard has three types of DCI formats with DCI format supporting two transport blocks, and is transmitted with different information bit numbers. Table II shows the DCI format of MHN-E.

One of the other features of the MHN-E system is that it has a different frame structure depending on the frequency sub-band. The MHN is capable of extending the frequency band based on a sub-band with a bandwidth of 125 MHz. Among them, the cell synchronization and the BCH signal are transmitted through the primary band. MHN-E is characterized by using a frame structure that eliminates the interference of synchronous signals and BCH signals between adjacent cells. That is, the adjacent two cells allocate the frequency resources of the synchronization signal and the BCH signal to different sub-bands, and the resources used by the neighboring cells are left empty and not used. This method minimizes the interference of adjacent cells in cell search and network connection process.

### B. Receiver algorithm

Since the MHN periodically transmits the cell-specific reference signal (CRS), the terminal uses the signal to estimate the wireless channel. In MHN, CRS is transmitted at intervals of four symbols among 0 to 39 OFDM symbols, and is transmitted every 6 subcarriers within one symbol. When the transmitted CRS signal in the  $i$ -th OFDM symbol of the  $p$ -th

antenna output from the base station is  $X_{i,k}^{(p)}$ , the received CRS signal can be written as follows.

$$\hat{Y}_{i,k}^{(p)} = H_{i,k}^{(p)} \cdot X_{i,k}^{(p)} + \hat{W}_{i,k}^{(p)}, \text{ for } p = \{0,1\} \quad (3)$$

where  $i = 0, 4, 8, \dots, 36$ . In (3),  $H_{i,k}^{(p)}$  represents wireless channel and  $\hat{W}_{i,k}^{(p)}$  represents noise component.

The constructed MHN-E TE uses a least squares (LS) scheme for channel estimation. The LS Estimator estimates the frequency response of the channel obtained by dividing the received signal by the transmitted M-CRS. The LS Estimate of the  $p$ -th receiving antenna, the  $i$ -th OFDM symbol,  $\hat{H}_{i,k}^{(p)}$ , is made by following calculation.

$$\hat{H}_{i,k}^{(p)} = \hat{Y}_{i,k}^{(p)} / X_{i,k}^{(p)} \quad (4)$$

$$i = 0, 4, 8, 12, 16, 20, 24, 28, 32, 36 \text{ if } p \in \{0,1\}$$

The CRS channel estimated for each subcarrier is interpolated to the entire frequency band using FFT. The channel estimation values of other OFDM symbols are obtained by linear interpolation between CRS symbols. The signal to noise ratio (SNR) can be calculated using the channel estimate of the CRS symbol.

The implemented channel equalizer generates the log likelihood ratio (LLR) using the Alamouti detector for the SFBC transmission mode and the minimum mean squared error (MMSE) algorithm for the SM mode and outputs it to the Turbo decoder.

### III. MHN-E TE PLATFORM

The MHN technology has already verified the technology using the 31 GHz frequency band [2]. In Korea, Flexible Access Common Spectrum (FACS) frequency of 24 ~ 26.5 GHz is now available and the system using that frequency will be built in Seoul subway. And if a company develops 20 to 40 GHz antennas and RF, MHN technology can be applied. For MHN-E prototype, the frequency of 25.5 GHz is chosen and up to 8 sub-bands can be used, and overall occupied bandwidth is 1 GHz.

The MHN-E TE consists of antennas, RF module, ADC / DAC, and a baseband board as shown in Fig 2. The physical layer functions are implemented in five FPGAs. In the figure, there is one TX antenna of TE and two RX antennas. The two RX antennas correspond to vertical polarization and horizontal polarization, respectively. The fabricated polarized antenna is designed with a cross polarization discrimination of 50dB. In Rep. of Korea, the radiation power of FACS is limited to 36 dBm, including 16 dBm of antenna gain. The half-power beamwidths (HPBW) of TX and RX antennas are equal to 20 and 8 degrees. However, the fabricated RU has 2 TX and 2 RX antenna, so, SISO, SFBC and 2x2 SM is capable in downlink.

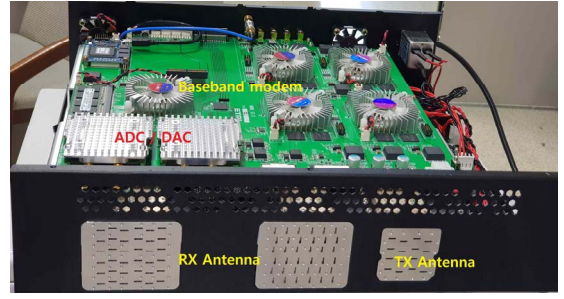


Fig. 2. System architecture of MHN-E.

### IV. LLR SIMULATION

The simulation of this paper is conducted by a fixed-point simulator, which was used as a basis for verification in hardware development. Therefore, the simulation results reflect the exact performance of the MHN-E system. This performance simulation result may indicate a channel quality indication (CQI). The CQI information is transmitted from the TE to the BS to set a modulation coding scheme (MCS). The MHN system sets 4 bits to use the CQI and transmits it on each uplink slot through the uplink control channel.

The simulation model for performance analysis is shown in Table III. The resource block is assumed to be 48 RB, and the QAM mapping and the coding rate are different according to the MCS. The wireless channel assumes only the line of sight and uses the AWGN channel. No frequency and time offsets are assumed. Because, the compensation by frequency tracking was performed at the RF module, and the time offset is assumed to be less than the guard interval of an OFDM symbol, which avoids timing shift due to incremental time offset.

In the MHN-E system, the antenna is oriented vertically and horizontally, but in the actual situation where the TE moves or there is a reflector in the periphery, there is an intersection component of the antenna. In the road test of this system, it was confirmed that the communication performance deteriorates due to the surrounding structure or vehicle while moving the MHN-E TE in the SM transmission mode. Therefore, this paper assumes the intersection component caused by the object adjacent to the receiving antenna in the presence of the LOS component and performs the simulation to analyze the effect. In the Table III, the crossover component is represented by  $\alpha$  of the channel matrix.

TABLE III. SUMMARY OF SIMULATION PARAMETERS

Parameters	Value
# Resource block	48
MCS (code rate)	19 (0.7)
Channel	AWGN
Channel matrix	$\begin{bmatrix} 1 & \alpha \\ \alpha & 1 \end{bmatrix}$ , $\alpha$ : correlation rate
Ant. Correlation rate	0, 0.2, 0.3, 0.5, 0.7
Mode	SFBC / Spatial multiplexing
Data rate per sub-band	285.46 Mbps / 571.92 Mbps

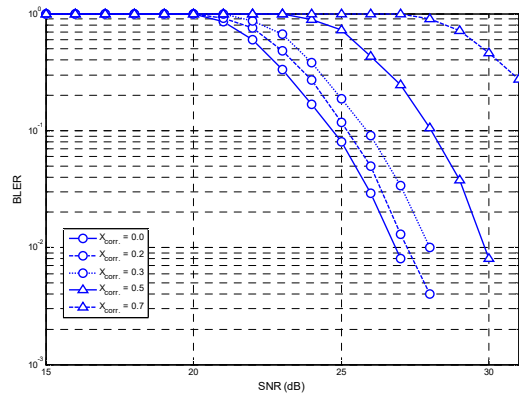


Fig. 3. Block error rate of 2x2 SM according to cross correlation rate

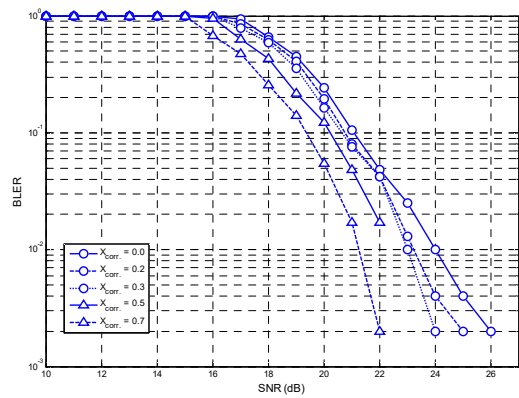


Fig. 4. Block error rate of SFBC according to cross correlation rate

Figures 3 and 4 show the simulation results of block error rate (BLER) versus signal to noise ratio (SNR) for 2x2 SM and SFBC transmission modes, respectively.

When the correlation rate is zero, the required SNR at BLER 0.01 is about 26.5 dB in the SM mode and 24 dB in the SFBC mode. Antenna diversity gain can be seen. In the SM mode, as the correlation rate between the antennas increases, the BLER deteriorates. An interference of 0.5 or more leads to a large performance deterioration. On the other hand, in the case of the SFBC mode, the higher the correlation rate, the better the demodulation performance, which shows the diversity effect using the two antennas. From these results, we can see that the SM mode will be work properly in low correlation rates.

Above link level simulation results can be used to signal the channel quality. For uplink signaling of CQI, we have simulated BLER versus SNR many times. The CQI value based on cross-permeation rate of 0.2 is obtained. Table IV shows the CQI table which maps a 4-bit CQI value to a modulation and coding scheme.

TABLE IV. CQI TABLE OF SM MODE

SNR	CQI	MCS	SNR	CQI	MCS
30	15	21	15	7	9
28	14	20	13	6	7
27	13	19	11	5	6
23	12	17	8	4	4
21	11	15	6	3	3
20	10	13	4	2	2
17	9	12	2	1	0
16	8	10	<2	0	x

## V. CONCLUSION

The MHN-E system supports a data rate of 1 Gbps or higher as a wireless backhaul for trains. Unlike conventional MHN, the MHN-E employs polarization MIMO to implement data multiplexing, thereby doubling the throughput. Recently, the platform of MHN-E system has been manufactured and proved its possibility. This paper shows the simulation results of the transmission performance of the MHN-E system. To this end, this paper has described the specifications of the MHN-E system and the algorithms for demodulation. The simulation results show the BLER according to the SNR when the MHN-E system uses SFBC and spatial multiplexing MIMO. Simulations were carried out to verify the performance of cross - polarized antennas. As expected, performance deterioration due to cross-permeation component was observed at 2x2 SM, but, under the low cross-permeation rate, the SM mode operates properly. The result of this paper was used to assign the possible MCS based on the BLER. The transmission of the correct CQI enables the downlink transmission rate to be adjusted according to the situation, thereby improving the overall data throughput.

## REFERENCES

- [1] H. S. Cheong et. al, "Trend analysis of Moving Wireless Backhaul Technologies for Mobile Hotspot Networks," *Electronics and Telecommunications Trend*, vol. 30, no. 1, pp. 12-20, Feb. 2015.
- [2] S. Choi, H. Chung, J. Kim, J. Ahn, and I. Kim, "Mobile hotspot network system for high-speed railway communications using millimeter waves," *ETRI J.*, vol. 38, no. 6, pp. 1052-1063, Dec. 2016.
- [3] H. Chung et al., "From architecture to field trial: a millimeter wave based MHN system for HST communications toward 5G," in *Proc. 2017 European Conference on Networks and Communications (EuCNC)*, Oulu, Finland, Jun. 12-15, 2017, pp. 1-5.
- [4] J. Kim, H. S. Chung, S. W. Choi, I. G. Kim, and Y. Han, "Mobile hotspot network enhancement system for high-speed railway communication," in *Proc. 2017 11th European Conference on Antennas and Propagation (EuCAP)*, Paris, France, Mar. 19-24, 2017, pp. 2885-2889.
- [5] G. Noh, J. Kim, H. S. Chung, B. Hui, Y. M. Choi, and I. Kim, "mmwavebased mobile backhaul transceiver for high speed train communication systems," in *Proc. 2017 IEEE Globecom Workshops (GC Wkshps)*, Singapore, Dec. 4-8, 2017, pp. 1-5.
- [6] S. Choi, I. G. Kim, D. J. Kim, "Uplink Pilot Signal Design for Mobile Wireless Backhaul," *J. Korean Inst. Commun. Inf. Sci.*, vol. 40, no. 6, pp. 1005-1013, 2015.
- [7] Jonathan Wells, *Multi-Gigabit Microwave and Millimeter-Wave Wireless Communications*. Artech House, 2010.